JOURNAL OF SOLID STATE CHEMISTRY 97, 332–339 (1992)

Framework Composed of Interconnected Quadruple-Octahedra Infinite Chains: Synthesis and Structure of Calcium Ytterbium Sulfide, $CaYb_2S_4$, with the Yb_3S_4-Type Structure

JAMES D. CARPENTER AND SHIOU-JYH HWU*

Department of Chemistry, Rice University, P.O. Box 1892, Houston, Texas 77251

Received August 13, 1991; in revised form October 7, 1991

Single crystals of the ternary calcium ytterbium compound, $CaYb_2S_4$, have been synthesized using an eutectic, halide flux and have been structurally characterized by the X-ray single-crystal diffraction method. The compound crystallizes in an orthorhombic unit cell, *Pnma* (No. 62), with cell dimensions of $a = 12.807\ (3)$ Å, $b = 3.836\ (2)$ Å, $c = 12.964\ (3)$ Å, $V = 636.9\ (7)$ Å^3, and $Z = 4$. The least-squares refinement of 658 observed reflections (with $F_0^2 > 3\,\sigma\,(F_0^2)$) gives a final structure solution of $R = 0.026$, $R_w = 0.030$, and GOF = 1.06 for 45 variables. This compound has adopted a Yb_3S_4-type structure in which the 7-coordinated divalent Yb^{2+} sites are occupied by Ca^{2+} cations. The refined occupancy factor on the calcium site suggests some nonstoichiometry, which is attributed to the solid solution of a ytterbium-rich phase. The crystal formula found is $Ca_{1-x}Yb_{2+x}S_4$ ($x = 0.04$). The $CaYb_2S_4$ structure is a three-dimensional lattice which consists of interconnected quadruple-octahedra infinite chains. Each quadruple chain is built up from four edge-sharing octahedra that are composed of two pairs of asymmetric $Yb(1)S_6$ and $Yb(2)S_6$ groups. Structure comparison with another ternary rare-earth sulfide bearing a larger alkaline earth metal cation, $BaSm_2S_4$ ($CaFe_2O_4$-type), gives rise to some important insight for structure formation of rare-earth chalcogenide compounds.

Introduction

Crystallographic studies of ternary rare-earth chalcogenide compounds allow the role of cations, governing the structure formation, to be revealed. Patrie *et al.* (*1*, *2*) synthesized a series of ternary rare-earth chalcogenides with a general formula of $A(RE)_2Q_4$, where A = Ca, Sr, Ba; RE = Y, La, Ce–Lu; and Q = S, Se. In their studies, a number of interesting structure types are found to be interrelated to the size of cations, including both A-site and RE cations, as well as the reaction temperature (*3*). For strontium and barium compounds, the adopted structure types, Th_3P_4 and $CaFe_2O_4$, evidently depend solely upon the size of the rare-earth cations. The Th_3P_4-type is adopted by the early rare-earth compounds where RE = Ce–Gd for A = Sr and RE = Ce–Nd for A = Ba while the $CaFe_2O_4$-type structure is adopted by the sulfides and selenides of the late rare-earth compounds where RE = Tb–Lu for A = Sr and RE = Nd–Lu for A = Ba. The single crystal structure of $BaSm_2S_4$ ($CaFe_2O_4$-type) has recently been determined (*4*) and shows that the A-site cation (Ba) is 8-coordinated and the RE cation (Sm) is 6, while each sulfur is 5-coordinated with two barium

* To whom correspondence should be addressed.

0022-4596/92 $3.00

and three samarium atoms. In compounds adopting the structure of Th_3P_4, both A-site and early RE atoms are presumably 8-coordinated with respect to chalcogenide atoms (S and Se). As to the calcium series, $Ca(RE)_2S_4$, the observed structure types are complicated by three polymorphs, e.g., low-temperature Yb_3S_4-type (orthorhombic) (*5*), high-temperature $MnYb_2S_4$-type (orthorhombic) (*6*), and Th_3P_4-type (cubic) (*7*) structures. The orthorhombic structure types are adopted by RE = Ho–Lu and Y (except the high-temperature form of the Ho compound), while the cubic structure type is adopted by RE = Ce–Dy (and the high-temperature form of $CaHo_2S_4$). Due to a lack of single crystals, all structural characterization done so far has been by X-ray powder diffraction patterns. Using an eutectic, halide flux, a large number of needle-shaped crystals of the title compound can be synthesized. In this paper, we report the synthesis and the X-ray single crystal structure of $CaYb_2S_4$. The structure comparison between $CaYb_2S_4$ (Yb_3S_4-type) and $BaSm_2S_4$ ($CaFe_2O_4$-type) is also discussed.

Experimental

Synthesis and crystal growth. Single crystals of $CaYb_2S_4$ were discovered in the reaction products formed during an attempt to synthesize the "$CaYbSbS_4$" analogue of $CaYbInQ_4$ (Q = S, Se) (*8*) in a halide flux. For the preparation of the quaternary precursor a solid state reaction, using the starting materials CaS (Aesar, 99.99%), Yb (Aldrich, 99.9%), Sb (Aldrich, 99.999%), and S (Aldrich 99.99%) in a molar ratio of 1 : 1 : 1 : 3, was carried out. The reaction mixture was ground together under a blanket of nitrogen in a dry box and then loaded into a quartz reaction ampule, which was subsequently sealed under vacuum. The reaction mixture was heated at a rate of 30°C per hour to a final temperature of 950°C, annealed at this temperature for 3 days, and then cooled to room temperature over a 24-hr period. To prepare the flux, $CaCl_2$ (Johnson Mathey Inc., reagent) and KCl (Baker, reagent) were dried under vacuum at approximately 200°C, weighed in a dry box, and ground together prior to use. The composition of the eutectic flux was $CaCl_2$/KCl, ~74/26 mole % (mp, 640°C) (*9*). Crystal growth experiments were carried out in carbon-coated silica ampules, which were previously outgassed under vacuum. The ampules were loaded in a dry box with a mixture of the precursor and flux in a ratio of 1 : 4. The loaded ampules were held under active vacuum for 2.5 hr prior to sealing. The crystal growth reaction mixture was heated to 995°C at a rate of approximately 30°C per hour, held at 995°C for 6 days, cooled at a rate of 1.5°C per hour to 600°C, and then cooled to room temperature over a 24-hr period. Brownish-orange, transparent needle crystals of $CaYb_2S_4$ were isolated from the flux by washing the product with deionized water. (The major by-product is Sb_2S_3 according to powder X-ray diffraction patterns.)

Both $CaYb_2S_4$ and $BaSm_2S_4$ were examined by infrared spectroscopy. Diffuse reflectance infrared Fourier transform spectroscopy (DRIFTS) experiments were carried out using an IBM-98 FT-IR spectrometer (4000–600 cm^{-1}). A Spectratech IR-Plan spectrometer was used for single-crystal transmittance investigations (5000–500 cm^{-1}). The results from these investigations reveal that both phases are transparent in the infrared region.

Structure determination. A needle-shaped crystal, with dimensions 0.4 × 0.1 × 0.1 mm, was selected for indexing and intensity data collection. Diffraction data were collected using a Rigaku AFC5S four-circle diffractometer equipped with a graphite monochromator. The unit cell parameters and the orientation matrix for data collection were determined by least-squares fit of 25 peak maxima ($7.00 < 2\theta < 25.0$). There

was no detectable decay of the intensities of three standard reflections (2, 0, 3; −1, 0, 5; 1, 2, 1) which were measured every 150 reflections during data collection. The crystallographic data are listed in Table I. The TEXSAN software package (*10*) was used for the crystal structure solution and refinement. Data reduction, intensity analysis, and space group determination were accomplished with the program PROCESS. On the basis of the intensity statistics as well as the successful solution and structure refinement, the space group was determined to be *Pnma* (No. 62). Lorentz-polarization and empirical absorption corrections, based on two azimuthal scans (2θ = 21.35° and 34.34°), were applied to the intensity data. The atomic coordinates were found using the program SHELXS (*11*). The structure and thermal parameters were then refined by full-matrix least-squares methods based on F^2 to R = 0.027, R_w = 0.032, and GOF = 1.10. The occupancy factors for calcium and ytterbium atoms were initially refined, but the resultant values indicated nonstoichiometry only on the calcium site. The final refinement with the varied occupancy factor for calcium atoms results in improved values of R = 0.026, R_w = 0.030, and GOF = 1.06. A correction for secondary extinction (3.66(2) × 10^{-7}) was applied. The final positional and thermal parameters are given in Table II.

TABLE I

CRYSTALLOGRAPHIC DATA FOR $Ca_{1-x}Yb_{2+x}S_4$ (x = 0.04)

Formula mass (amu)	519.72
Space group	*Pnma* (No. 62)
Cell parameters[a]	
a (Å)	12.807(3)
b (Å)	3.836(2)
c (Å)	12.964(3)
V (Å^3)	636.9(7)
Z	4
T (K) of data collection	296
ρ calculated (g cm^{-3})	5.42
Radiation (graphite monochromated)	Mo$K\alpha$ (λ = 0.71069 Å)
Crystal shape, color	Needle, brownish-orange
Crystal size (mm)	0.4 × 0.1 × 0.1
Linear absorption coefficient (cm^{-1})	310.38
Transmission factors	0.83 to 1.00
Scan type	ω-scan
Scan speed (degrees min^{-1})	4.0
Scan range (degrees)	−0.45 to 0.45 in ω
Background counts	¼ of scan range on each side of reflection
2θ (max)	55°
Data collected	$+h$, $+k$, $\pm l$
p for σ (F^2)	0.03
No. of reflections measured ($F_0^2 > 0$)	1744
No. of reflections observed ($F_0^2 > 3\sigma(F_0^2)$)	1289
No. of unique reflections ($F_0^2 > 3\sigma(F_0^2)$)	658
F_{000}	896
$R(F^2)$	0.026
$R_w(F^2)$	0.030
R (on F for $F_0^2 > 3\sigma(F_0^2)$)	0.026
Goodness of fit	1.06
Extinction coefficient (×10^{-7})	3.67
No. of variables	45

[a] The refinement of cell constants is constrained in the orthorhombic crystal system.

TABLE II

POSITIONAL[a] AND THERMAL PARAMETERS FOR $CaYb_2S_4$

	x	z	$B_{(eq)}$[b]
Ca[c]	0.1316(2)	0.4164(2)	0.8(1)[d]
Yb(1)	0.35301(4)	0.20255(4)	0.62(2)
Yb(2)	0.39309(4)	0.58312(5)	0.68(2)
S(1)	0.0307(3)	0.6184(3)	0.7(1)
S(2)	0.2829(3)	0.7616(3)	0.8(1)
S(3)	0.2420(2)	0.0269(2)	0.7(1)
S(4)	0.4666(3)	0.3821(2)	0.7(1)

[a] y = ¼.
[b] Anisotropically refined atoms are given in the form of the isotropic equivalent displacement parameters defined as B_{eq} = $(8\pi^2/3)$ trace U.
[c] Refined occupance factor is 0.547(4) (see text).
[d] For comparison, the refined B_{eq} is 0.36(7) with a fixed occupancy factor (0.50).

Structure Description and Discussion

In compounds of $Ca(RE)_2S_4$ some solid solutions, extended by addition of rare-earth sesquisulfides, are reportedly known (*2*). This phenomenon is particularly appreciable for the calcium ytterbium sulfide compound $Ca_{1-x}Yb_{2+x}S_4$. It is important to know that before this report, no conclusion had been made on whether the nonstoichiometry is due to a cation defect on the Ca

site or due to mixed cations, such as $Ca^{2+}_{1-x}Yb^{2+}_x$. The occupancy factor for the calcium atoms is refined to be 0.55 (vs 0.50 for a fully occupied atom). Based upon this value, we suggest that the nonstoichiometry is due to the mixing of Yb^{2+} cations on Ca^{2+} sites. The calculated structure formula for the title compound is $(Ca_{0.96}Yb_{0.04})Yb_{2.00}S_4$ with $x = 0.04$. For the convenience of structural illustration the stoichiometric structure formula, $CaYb_2S_4$, is used hereafter.

The title compound crystallizes in an orthorhombic unit cell which contains four asymmetric units. This ternary calcium ytterbium sulfide, $CaYb_2S_4$, has the Yb_3S_4-type ($\equiv Yb^{2+}Yb^{3+}_2S_4$) structure with Ca^{2+} cations in positions of 7-coordination (Yb^{2+}-site) and Yb^{3+} cations in positions of 6-coordination. Figure 1 shows the contents of an unit cell structure as viewed approximately along the *b* axis. The unit cell is slightly tilted so that the octahedrally coordinated YbS_6 may be discerned. The two asymmetric $Yb(1)S_6$ and $Yb(2)S_6$ octahedra are found in a four (quadruple)-YbS_6 octahedral unit. This unit is centered around the inversion center at $(\frac{1}{2}, \frac{1}{2}, \frac{1}{2})$ with a set of two asymmetric YbS_6 octahedra on each side. The quadruple-octahedral building units share sulfur atoms, S(4)'s, to form an extended structure along the *ac* plane. The divalent cation Ca^{2+} is accommodated between the building units. In Fig. 1. the coordination of calcium, 7, is outlined by dashed lines.

Calcium and its coordinated sulfur atoms form a CaS_7 polyhedron. The geometry of this polyhedron can be best described as a

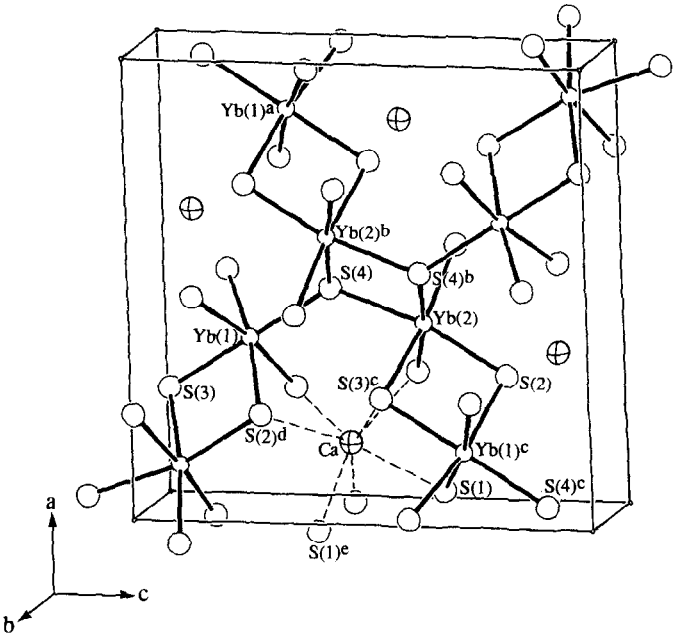

FIG. 1. The ORTEP drawing of the $CaYb_2S_4$ structure viewed approximately along the *b* axis. All the ytterbium atoms (in small open circles) occur at the mirror planes at $y = \frac{1}{4}$ and $\frac{3}{4}$. The completed YbS_6 octahedral coordination is shown with the sulfur atoms (large open circles) at $\pm\frac{1}{2}$ and $+\frac{1}{4}$ in *y* with respect to the ytterbium atoms. The four calcium atoms in the unit cell are shown in crosshatched circles. Atoms are labeled according to the asymmetric unit reported in Table II and the extra symmetry codes–a: $\frac{1}{2} + x, \frac{1}{4}, \frac{1}{2} - z$; b: $1 - x, \frac{3}{4}, 1 - z$; c: $\frac{1}{2} - x, \frac{3}{4}, \frac{1}{2} + z$; d: $\frac{1}{2} - x, \frac{3}{4}, -\frac{1}{2} + z$; e: $-x, \frac{3}{4}, 1 - z$.

monocapped trigonal prism (mTP) with six sulfurs forming a TP while the seventh is on the same mirror plane as the calcium atom, as shown in Fig. 2. The calcium atom is slightly off the center of the TP, which is attributed to the additional coordination on one side of the prism. That is to say the two equivalent Ca–S(2) bonds (above and below the mirror plane) adopt the longest bond distances, e.g., 2.983 (2) Å, due to the strong interaction with the monocapped sulfur, e.g., 2.923 (3) Å for Ca–S(1), in the opposite direction. Otherwise, the Ca–S distances are in the range of 2.86–2.98 Å (Table III), which is consistent with the crystal radii sum, 2.90 Å, of the 7-coordinated Ca^{2+} (1.20 Å) and 6-coordinated S^{2-} (1.70 Å), according to Shannon (*12*).

An ORTEP drawing of the above discussed quadruple-octahedral unit, Yb_4S_{18}, is shown in Fig. 3. As mentioned above, the octahedrally coordinated YbS_6 groups are adopted by two pairs of asymmetric $Yb(1)S_6$ and $Yb(2)S_6$ units which are connected

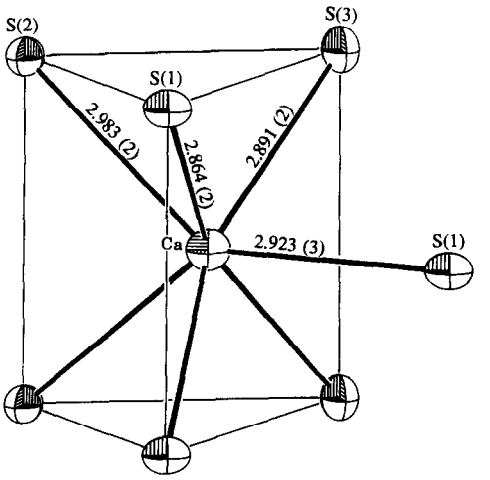

FIG. 2. The ORTEP drawing of the CaS_7 polyhedron is shown in a singly capped trigonal prismatic configuration. The anisotropic atoms are presented in 90% probability. The Ca–S bond lengths are given in angstroms.

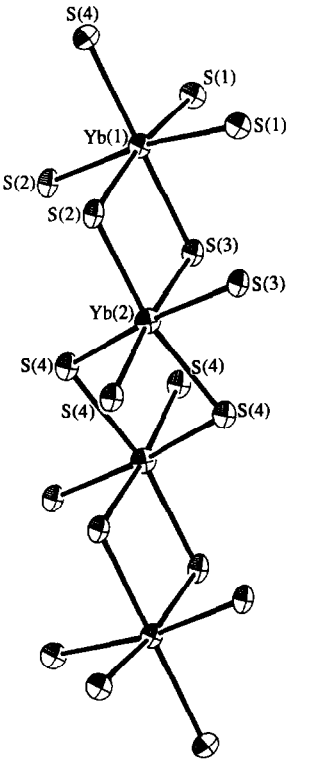

FIG. 3. The ORTEP drawing of the quadruple-octahedral unit, Yb_4S_{18}. The anisotropic atoms are presented in 95% probability. An inversion center occurs at the midpoint of the 4S(4) located at the middle of the drawing.

through sulfur atoms, i.e., S(2) and S(3) for $Yb(1)S_6$–$Yb(2)S_6$ and 2 × S(4) for $Yb(2)S_6$–$Yb(2)S_6$. The structure formula Yb_4S_{18} can be rewritten as $[Yb(1)S_{4/1}S_{2/2}]_2[Yb(2)S_{4/2}S_{2/1}]_2 \equiv [Yb(1)_2S_{10}][Yb(2)_2S_8]$. The Yb–S bond distances, as listed in Table IV, range from 2.66 to 2.78 Å, which is comparable with those observed in Yb_3S_4, e.g., 2.64–2.71 Å (*5*). They are also consistent with the sum, 2.71 Å, of the Shannon crystal radii of 6-coordinated Yb^{3+}, 1.008 Å, and S^{2-}, 1.70 Å (*12*). Based upon the octahedral angles of the two YbS_6 units, it is noted that both YbS_6 octahedral units are slightly distorted.

It is interesting to see that the structure

of the quadruple-octahedra unit, Yb_4S_{18}, is further extended along the *b* axis to form an infinite quadruple-octahedra chain. Figure 4 shows a partial structure of the infinite chain propagated along the [010] direction. The pseudo-threefold axis of each octahedron, as imagined, is situated in an approximately perpendicular direction with respect to the [010] direction. The $Yb(2)S_6$ octahedra share 6 of their 12 edges with the neighboring YbS_6 octahedra, while the $Yb(1)S_6$ octahedra share 4. This quadruple-octahedra infinite chain can be viewed as four YbS_6 octahedral layers in the sequence of $Yb(1)S_6$–$Yb(2)S_6$–$Yb(2)S_6$–$Yb(1)S_6$. In each layer the infinite chain is built up from YbS_6 octahedra sharing opposite (*trans*) edges, while the stacked layers share *cis* edges of the YbS_6 octahedra.

The structure of $CaYb_2S_4$ bears considerable similarity to $BaSm_2S_4$ in that it too exhibits fused infinite octahedral chains. Figure 5 compares the $CaYb_2S_4$ and $BaSm_2S_4$ structures, which are projected along the short *b* axes, with $(RE)S_6$ octahedra in shaded polyhedral representations. The structure building units are four edge-shared $(RE)S_6$ octahedra vs two, in length, respectively. The currently studied structure shows that the quadruple-octahedra units are linked together through octahedral corners, S(4), at the end and midway (waist) of the neighboring quadruple units. In $BaSm_2S_4$, however, the double-octahedra units are joined together exclusively through corner-sharing of the octahedral sulfurs. Furthermore, the immediate neigh-

TABLE III

IMPORTANT BOND DISTANCES (Å) AND ANGLES (DEGREES) FOR THE CaS_7 POLYHEDRON IN $CaYb_2S_4$

Ca^f–$S(1)^f$	2.921(4)	
Ca^f–$S(1)^{j,k}$	2.864(3)	(2×)
Ca^f–$S(2)^{d,g}$	2.984(3)	(2×)
Ca^f–$S(3)^{c,h}$	2.889(3)	(2×)
$S(1)^f$ –Ca^f–$S(1)^{j,k}$	79.64(1)	(2×)
$S(1)^j$ –Ca^f–$S(1)^k$	84.1(1)	
$S(1)^{j/k}$–Ca^f–$S(2)^{g/d}$	74.32(9)	(2×)
$S(1)^f$ –Ca^f–$S(3)^{c,h}$	78.67(10)	(2×)
$S(1)^{j/k}$–Ca^f–$S(3)^{c/h}$	92.30(7)	(2×)
$S(2)^g$ –Ca^f–$S(2)^d$	79.98(10)	
$S(2)^{d/g}$–Ca^f–$S(3)^{c/h}$	72.62(9)	(2×)
$S(3)^h$ –Ca^f–$S(3)^c$	83.2(1)	
$S(1)^f$ –Ca^f–$S(2)^{d,g}$	139.95(5)	(2×)
$S(1)^{j/k}$–Ca^f–$S(2)^{d/g}$	126.2(1)	(2×)
$S(1)^{j/k}$–Ca^f–$S(3)^{c/h}$	158.33(1)	(2×)
$S(2)^{d/g}$–Ca^f–$S(3)^{h/c}$	123.57(1)	(2×)

Note. Additional symmetry codes–j: $-x$, $-\frac{1}{2}+y$, $1-z$; k: $-x$, $\frac{1}{2}+y$, $1-z$.

TABLE IV

IMPORTANT BOND DISTANCES (Å) AND ANGLES (DEGREES) FOR YbS_6 OCTAHEDRA IN $CaYb_2S_4$

$Yb(1)S_6$ octahedron		
$Yb(1)^f$–$S(1)^{d,g}$	2.662(2)	(2×)
$Yb(1)^f$–$S(2)^{d,g}$	2.701(3)	(2×)
$Yb(1)^f$–$S(3)^f$	2.685(3)	
$Yb(1)^f$–$S(4)^f$	2.744(3)	
$S(1)^g$ –$Yb(1)^f$–$S(1)^d$	92.2(1)	
$S(1)^{d/g}$–$Yb(1)^f$–$S(2)^{d/g}$	88.01(8)	(2×)
$S(1)^{d,g}$–$Yb(1)^f$–$S(3)^f$	87.07(9)	(2×)
$S(1)^{d,g}$–$Yb(1)^f$–$S(4)^f$	92.9(9)	(2×)
$S(2)^g$ –$Yb(1)^f$–$S(2)^d$	90.5(1)	
$S(2)^{d,g}$–$Yb(1)^f$–$S(3)^f$	84.21(9)	(2×)
$S(2)^{d,g}$–$Yb(1)^f$–$S(4)^f$	95.82(9)	(2×)
$S(1)^{d/g}$–$Yb(1)^f$–$S(2)^{g/d}$	171.3(1)	(2×)
$S(3)^f$ –$Yb(1)^f$–$S(4)^f$	179.96(10)	(2×)
$Yb(2)S_6$ octahedron		
$Yb(2)^f$–$S(2)^f$	2.710(4)	
$Yb(2)^f$–$S(3)^{c,h}$	2.684(2)	(2×)
$Yb(2)^f$–$S(4)^{b,i}$	2.667(2)	(2×)
$Yb(2)^f$–$S(4)^f$	2.772(3)	
$S(2)^f$ –$Yb(2)^f$–$S(3)^{c,h}$	84.05(9)	(2×)
$S(2)^f$ –$Yb(2)^f$–$S(4)^{b,i}$	101.91(9)	(2×)
$S(3)^h$ –$Yb(2)^f$–$S(3)^c$	91.2(1)	(2×)
$S(3)^{c,h}$–$Yb(2)^f$–$S(4)^f$	87.90(8)	(2×)
$S(3)^{c/h}$–$Yb(2)^f$–$S(4)^{b/i}$	88.08(8)	(2×)
$S(4)^f$ –$Yb(2)^f$–$S(4)^{b,i}$	86.01(9)	(2×)
$S(4)^b$ –$Yb(2)^f$–$S(4)^b$	91.97(10)	
$S(2)^f$ –$Yb(2)^f$–$S(4)^f$	168.48(10)	
$S(3)^{c/h}$–$Yb(2)^f$–$S(4)^{i/b}$	173.89(10)	(2×)

Note. The shortest sulfur to sulfur distance is S(2)–S(3), 3.479(5) Å. Symmetry codes–f: x, y, z; g: $\frac{1}{2}-x$, $-y$, $-\frac{1}{2}+z$; h: $\frac{1}{2}-x$, $-y$, $\frac{1}{2}+z$; i: $1-x$, $-\frac{1}{2}+y$, $1-z$; also see Fig. 1 for the additional symmetry codes.

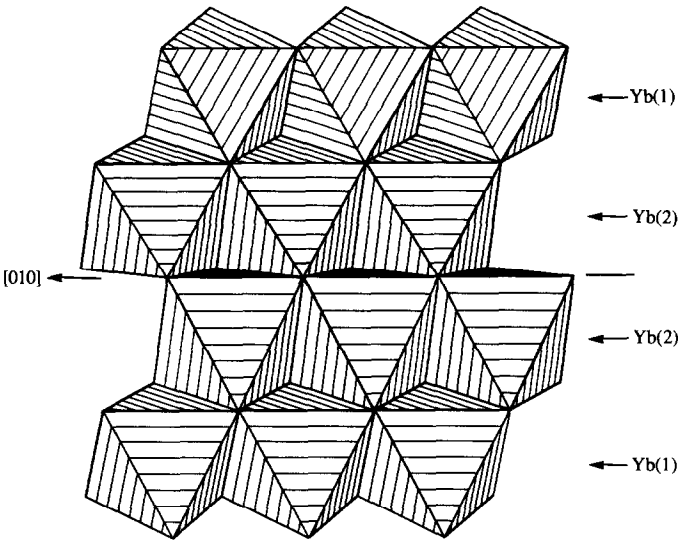

FIG. 4. A partial structure of the Yb_4S_{18} quadruple-octahedral infinite chain, as shown by three pairs of four YbS_6 octahedra, is plotted along the [010] direction.

bors of the quadruple units in $CaYb_2S_4$ are related by *n*-glide planes perpendicular to *a* at $x = \frac{1}{4}$ and $\frac{3}{4}$, while the neighboring double units in $BaSm_2S_4$ are asymmetrical. Nevertheless, both structures are composed of fused $(RE)S_6$ octahedra, each of which is bound to four other units.

A simple explanation can be discerned for the change from two- to four-fused $(RE)S_6$ octahedra in each building unit, the reduction in size of the *A*-site cations, e.g., 1.56 Å for the 8-coordinated Ba^{2+} cation compared with 1.20 and 1.26 Å for the 7- and 8-coordinated Ca^{2+} cation, respectively (*12*). The

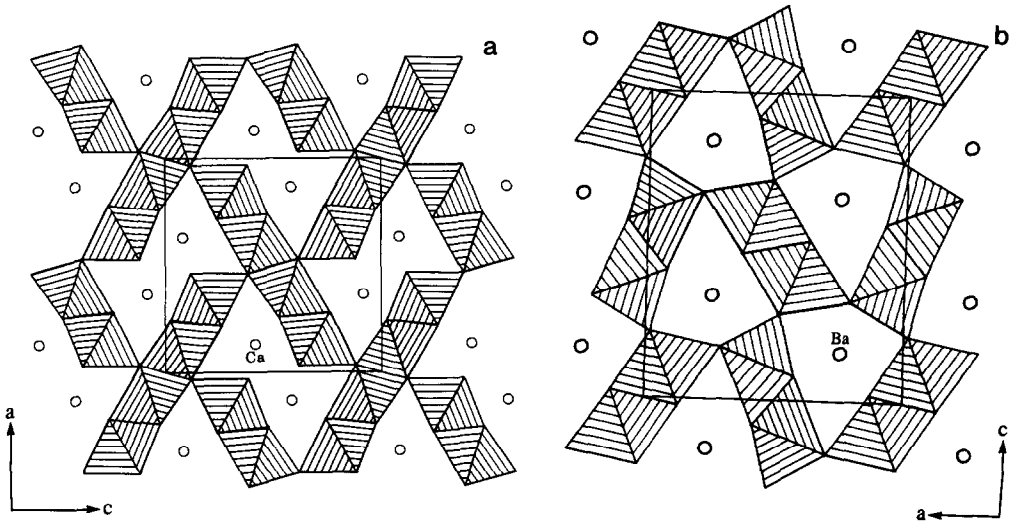

FIG. 5. Comparison of the (a) $CaYb_2S_4$ (Yb_3S_4-type) and (b) $BaSm_2S_4$ ($CaFe_2O_4$-type) structures in the STRUPLO polyhedral representations projected along the *b* axis.

pseudo-triangular channels formed by corner-sharing double-octahedra units are apparently too large to contain a much smaller calcium cation. Alternatively, the three-dimensional framework of the title compound provides interconnected double, pseudo-triangular channels where the small electropositive cations (Ca^{2+}) reside. The size of the calcium atom, therefore, is an important factor in the formation of the Yb_3S_4-type structure.

Another important feature in differentiating the structures of $CaYb_2S_4$ and $BaSm_2S_4$ is the variation in sulfur-to-cation interactions. In the barium compound, each sulfur atom is equally coordinated with three samarium and two barium atoms. However, the coordination of the sulfur atoms in $CaYb_2S_4$ is inhomogeneous, e.g., S(1) is 5-coordinated with three calcium and two ytterbium cations, S(2) and S(3) are 5-coordinated but with two calcium and three ytterbium atoms, while S(4) is only 4-coordinated with purely ytterbium atoms. This is believed to be attributed to the change in coordination number with respect to the A-site cations, Ca^{2+} (7) and Ba^{2+} (8).

In conclusion, this difference in connectivity of the $(RE)S_6$ octahedra and the configuration of the AS_n polyhedra in the $A(RE)_2S_4$ series is attributed to the structural framework accommodation of the size differences in electropositive cations. Also, it is important to note that $CaYb_2S_4$ possess nonstoichiometry which is attributed to the solid solution of a ytterbium-rich phase. This nonstoichiometry results in a calculated structure formula for the title compound of $Ca_{1-x}Yb_{2+x}S_4$ ($x = 0.04$).

Acknowledgments

This research was supported by the Robert A. Welch Foundation and in part by a Rice University start-up grant. The authors are indebted to Mr. Z Xiao for the DRIFTS experiments and to Dr. S. Hsu (Shell, Westhallow Research Center) for single crystal IR spectroscopy. Financial support for the single crystal X-ray diffractometer by the National Science Foundation is gratefully acknowledged.

References

1. M. Patrie, S. M. Golabi, J. Flahaut, and L. Domange, *C.R. Acad. Sci. Paris* **259,** 4039 (1964).
2. M. Patrie, J. Flahaut, and G. Chaudron, *C.R. Acad. Sci. Paris* **264,** 395 (1967).
3. J. Flahaut, *in* "Progress in the Science and Technology of the Rare Earths," Vol. 3, pp. 209–283, Pergamon, Elmsford, NY (1968).
4. J. D. Carpenter and S.-J. Hwu, *Acta Crystallogr. Sect. C,* in press.
5. R. Chevalier, P. Laruelle, and J. Flahaut, *Bull. Soc. Fr. Mineral. Cristallogr.* **90,** 564 (1967).
6. H. H. Heikens, R. S. Kuindersma, C. F. van Bruggen, and C. Haas, *Phys. Status Solidi A* **46,** 687 (1978).
7. K. Meisel, *Z. Anorg. Allg. Chem.* **240,** 300 (1939).
8. J. D. Carpenter and S.-J. Hwu, submitted for publication.
9. E. M. Levin and H. F. McMurdie (Eds.), "Phase Diagrams for Ceramists," Vol. II, Fig. 3054, The American Ceramic Society, Columbus, OH (1969).
10. "TEXSAN: Single Crystal Structure Analysis Software, Version 5.0," Molecular Structure Corp., The Woodlands, TX (1989).
11. G. M. Sheldrick, *in* "Crystallographic Computing 3" (G. M. Sheldrick, C. Krüger, and R. Godard, Eds.), pp. 175–189, Oxford Univ. Press, London/New York (1985).
12. R. D. Shannon, *Acta Crystallogr. Sect. A* **32,** 751 (1976).